



1 **Ensemble cloud-resolving modelling of a historic back-building mesoscale**
2 **convective system over Liguria: The San Fruttuoso case of 1915**

3

4 Antonio Parodi¹, Luca Ferraris^{1,2}, William Gallus³, Maurizio Maugeri⁴, Luca Molini¹, Franco
5 Siccardi¹, and Giorgio Boni^{1,2}

6

7 1- CIMA Research Foundation, Savona, Italy

8 2- Dipartimento di Informatica, Bioingegneria, Robotica e Ingegneria dei Sistemi,

9 University of Genoa, 16145 Genoa, Italy

10 3- Department of Geological and Atmospheric Sciences, Iowa State University, Ames, Iowa

11 4- Università degli Studi di Milano, Dipartimento di Fisica, Milan, Italy

12

13 **Abstract**

14 Highly localized and persistent back-building mesoscale convective systems represent
15 one of the most dangerous flash-flood producing storms in the north-western
16 Mediterranean area. Substantial warming of the Mediterranean Sea in recent decades
17 raises concerns over possible increases in frequency or intensity of these types of
18 events as increased atmospheric temperatures generally support increases in water
19 vapor content. However, analyses of the historical record do not provide a univocal
20 answer, but these are likely affected by a lack of detailed observations for older
21 events.

22 In the present study, 20th Century Reanalysis Project initial and boundary condition
23 data in ensemble mode are used to address the feasibility of performing cloud-
24 resolving simulations with 1 km horizontal grid spacing of a historic extreme event
25 that occurred over Liguria: The San Fruttuoso case of 1915. The proposed approach
26 focuses on the ensemble Weather Research and Forecasting (WRF) model runs that
27 show strong convergence over the Liguria sea, as these runs are the ones most likely
28 to best simulate the event. It is found that these WRF runs generally do show wind
29 and precipitation fields that are consistent with the occurrence of highly localized and
30 persistent back-building mesoscale convective systems, although precipitation peak
31 amounts are underestimated. Systematic small north-westward position errors with
32 regard to the heaviest rain and strongest convergence areas imply that the Reanalysis
33 members may not be adequately representing the amount of cool air over the Po Plain
34 outflowing into the Liguria Sea through the Apennines gap. Regarding the role of
35 historical data sources, this study shows that in addition to Reanalysis products,
36 unconventional data, such as historical meteorological bulletins newspapers and even
37 photographs can be very valuable sources of knowledge in the reconstruction of past
38 extreme events.

39



40 1. Introduction

41 Flash floods are phenomena very common to most Mediterranean coastal cities,
42 accountable for millions of euros of damage and tens to hundreds of victims every
43 year (Gaume et al. 2009). The north-western Mediterranean area is affected by such
44 events in a period usually spanning from late summer (the end of August) to late fall
45 (early December): in this period, the warm waters of the sea, in combination with
46 large-scale meteorological systems coming from the Atlantic Ocean, provide a huge
47 amount of energy, namely latent and sensible heat fluxes, to the atmosphere (Boni et
48 al. 2006, Reale et al. 2011, Pinto et al. 2013). Heavy precipitation is then triggered by
49 the typically very steep topography of the coasts: it is frequent to observe the
50 monthly average rainfall to fall intensely in just a few hours and/or a significant
51 fraction (up to 30-40%) of the yearly average in one day (Parodi et al 2012, Fiori et
52 al. 2014). Obviously, the losses experienced in terms of human lives and economic
53 damage in these very densely populated areas are often dramatic.

54 Among the flash flood producing storms in the Mediterranean area, a prominent
55 feature is the highly localized and persistent back-building of mesoscale convective
56 systems (MCSs, Schumacher and Johnson 2005, Duffourg et al. 2015, Violante et al.
57 2016). Such a scenario has been observed often in the last decade, when Liguria (NW
58 Italy) and Southern France have been repeatedly hit by severe floods: 2010 Varazze
59 and Sestri Ponente, 2011 Cinqueterre and Genoa, 2012 Marseille and Isle du Levant,
60 2014 Genoa and Chiavari, 2015 Nice. As shown in several recent works (Parodi et al.
61 2012, Rebora et al. 2013, Fiori et al. 2014, Duffourg et al 2015, Silvestro et al. 2015,
62 Cassola et al. 2016, Silvestro et al. 2016), convective cells, embedded in such MCSs,
63 are generated on the sea by the convergence of a warm and moist south-easterly flow
64 and a northerly much colder and drier one. These structures are then advected to the
65 land where the combined action of the aforementioned currents and the topography
66 force them to persist for several hours over a very localized area (e.g. about 100
67 km²).

68 Many flood frequency studies have been carried out, focusing on rainfall regimes and
69 Mediterranean flood seasonality and type (Barriendos et al. 2003, Llasat et al. 2005,
70 Barriendos et al. 2006, Boni et al. 2006, Pinto et al. 2013, Llasat et al. 2014, Toreti et
71 al. 2015). Due to the exploitation of both documentary sources and early
72 measurements, these analyses have been able to go back several centuries, however,
73 their results have been mostly inconclusive regarding changes in frequency of
74 occurrence. Well-defined trends have not been found as usually flood frequency
75 oscillates from period to period with no significant growth, not even in the most recent
76 decades, regardless of the event's duration (a few hours to days).

77 The same result applies to precipitation extremes and their possible changes over the
78 Mediterranean area in recent decades, studied by several authors, either by empirical
79 or (mainly at-site) extreme value theory approaches (see e.g. Brunetti et al., 2001,
80 2004, Alpert et al., 2002, Kostopoulou and Jones, 2005, Moberg et al., 2006, Brunet
81 et al., 2007, Kioutsioukis et al., 2010, Rodrigo, 2010, Toreti et al., 2010, van den
82 Besselaar et al., 2013). The temporal tendencies are not fully coherent throughout the
83 region (Ulbrich et al., 2012) and rather conditioned by the specific site, the approach
84 used and the period examined (Brugnara et al., 2012, Brunetti et al., 2012, Maugeri
85 et al., 2015). On the contrary, an increase in precipitation extremes over the
86 Mediterranean area is generally indicated by climate model scenarios (Alpert et al.,
87 2002, Giorgio and Lionello, 2008, Trenberth, 2011).



88 It is therefore still an open debate whether the frequency of these phenomena is
89 really increasing or if it is merely the perception of both the general public and
90 scientific community. The latter hypothesis is supported by the fact that in the last
91 10-20 years the observational capabilities have substantially increased. For example,
92 in Italy alone, the remotely automated weather station network has grown to 5000
93 stations offering an average density of about 1/75 station/km² with a 1 to 10-minute
94 sampling rate. At the same time, the national weather radar network reached a fully
95 operational coverage allowing for direct evaluation of the space-time structure of
96 precipitation (Rebora et al. 2012).

97 Other factors contributing to enhance the perception of an increasing frequency of
98 extreme precipitation and floods are that it has become much easier for weather-
99 related disasters to make it to the news (Pasquaré and Oppizzi 2012, Grasso and
100 Crisci 2016) and therefore to the general public, and that a rapidly growing population
101 and soil consumption increases the exposure of the population to such phenomena
102 (Ward et al. 2013, SOER 2015).

103 To better investigate whether extreme precipitation and flood frequency are really
104 increasing in the Mediterranean, it is important to improve the exploitation of the
105 information available from past meteorological data. A contribution to this
106 improvement may come from the development of methods that identify which
107 ensemble analyses from projects like the 20th Century Reanalysis Project are able to
108 produce precipitation fields that are reasonably intense and capable of causing
109 extreme floods.

110 This paper focuses on a case study with the aim of investigating the ability of cloud-
111 resolving grid spacing atmospheric simulations to capture the main features of an
112 event causing a very severe flash flood. These simulations are performed using the
113 Weather Research and Forecasting (WRF, Skamarock et al. 2005) numerical
114 meteorological model forced by an ensemble of reanalysis fields from the 20th Century
115 Reanalysis Project (Compo et al. 2006, Compo et al. 2011). The work is also
116 important to reveal how well fine-scale models can simulate an event for which
117 observations used to initialize the forcing model are extremely sparse (see section 4).
118 One prior work, Michaelis and Lackmann (2013), showed some promising results in
119 the use of WRF for another historical event, the New England Blizzard of 1888, but
120 that event was a midlatitude cyclone driven by dynamics on a larger-scale. More on
121 the windstorm modelling side, Stucki et al. (2015) reconstructed a 1925 high-impact
122 foehn storm in the Swiss Alps.

123 In this study, the case under investigation was a very intense flash-flood producing
124 event that occurred in 1915 in eastern Liguria (20-25 km east of Genoa, Liguria
125 region capital city), affecting San Fruttuoso, a small hamlet near Portofino, and the
126 coastal cities of Santa Margherita Ligure, Rapallo, and Chiavari (Figure 1). Based
127 on the newspapers of the time and documentary sources, after relatively light rain during
128 the night between September 24th and 25th, on the early morning of September 25th,
129 the area was hit for a few hours (7-11 UTC) by violent rain that triggered widespread
130 flash flooding, and a devastating debris flow. This landslide half-demolished the San
131 Fruttuoso thousand-year old abbey and laid down a thick layer of sand and rocks to
132 form a still existing 20-metre-wide 2-metre-deep beach (Faccini et al. 2008),
133 nowadays a very popular seaside resort. Based both on the observations of the time
134 (wind speed/direction, rainfall, observed lightnings) available for north-western Italy,
135 and on the model simulations, the occurrence of a back-building MCS is suggested.

136

137

Fig. 1



138 The paper is organized as follows. In Section 2 the 1915 convective event is
139 presented. Section 3 describes the WRF-ARW model setting performed. Results are
140 discussed in Section 4. Conclusions are drawn in Section 5.

141

142 **2. Meteorological scenario**

143 The synoptic and mesoscale information for this event are available both from the 20th
144 Century Reanalysis Project (Compo et al. 2006, Compo et al. 2011) and from the
145 weather bulletins issued on a daily basis by the Italian Royal Central Office for
146 Meteorology (Regio Ufficio Centrale di Meteorologia e Geodinamica).

147 The 20th Century Reanalysis Project is an effort led by the Earth System Research
148 Laboratory (ESRL) Physical Sciences Division (PSD) of the National Oceanic and
149 Atmospheric Administration (NOAA) and the Cooperative Institute for Research in
150 Environmental Sciences (CIRES) at the University of Colorado to produce a reanalysis
151 dataset covering the entire twentieth century, assimilating only surface observations
152 of synoptic pressure, monthly sea surface temperature and sea ice distribution. The
153 observations have been assembled through international cooperation under the
154 auspices of the Atmospheric Circulation Reconstructions over the Earth (ACRE)
155 initiative, and working groups of Global Climate Observing System (GCOS) and World
156 Climate Research Program (WCRP). The Project uses an Ensemble Filter data
157 assimilation method, which directly yields each six-hourly analysis as the most likely
158 state of the global atmosphere, and gives also estimates of the uncertainty in that
159 analysis. This dataset provides the first estimates of global tropospheric variability
160 spanning from 1851 to 2012 with a six-hourly temporal resolution and a 2.0° grid
161 spacing. This study adopts 20th Century Reanalysis Project version 2C, which uses the
162 same model as version 2 with new sea ice boundary conditions from the COBE-SST2
163 (Hirahara et al. 2014), new pentad Simple Ocean Data Assimilation with sparse input
164 (SODAsi.2) sea surface temperature fields (Giese et al. 2016), and additional
165 observations from ISPD version 3.2.9 (Cram et al. 2015, Compo et al. 2013, Hirahara
166 et al. 2014, Krueger et al. 2013, Whitaker et al. 2004).

167 The weather bulletins issued by the Italian Royal Central Office for Meteorology
168 include weather maps at 7 UTC and 20 UTC and data (sea level pressure, wind
169 (direction and speed), temperature, cloud cover, cloud direction, state of the sea,
170 weather of the past 24 hours and notes) from about 125 Italian stations.

171 According to the reanalysis fields, the baroclinic circulation over Europe at 6 UTC of
172 September 25th, (i.e. a few hours before the most intense phase of the event) is quite
173 typical for heavy precipitation events over the study area, with an upper-level trough
174 over Great Britain leading to a diffluent flow over the Liguria sea area, in combination
175 with a widespread high pressure block on eastern Europe and southern Russia (Fig.
176 2a). The diffluent flow over the Liguria sea area is associated with warm air advection
177 at 850 hPa from the southern Mediterranean towards northern-western Mediterranean
178 coastlines (Fig. 2c). Further information is provided by the mean sea level pressure
179 (MSLP) field at the European scale: both the reanalysis field (06 UTC, Fig. 2b) and the
180 Italian weather map (7 UTC, Fig. 3) show an elongated trough over the western
181 Mediterranean and a prominent ridge over south-eastern Europe, representing a
182 blocking condition on the large-scale. The Italian weather map gives also evidence of
183 a significant surface pressure gradient between the Po Valley and the Liguria sea.

184

Fig. 2

185

Fig. 3

186 On the mesoscale, at 06 UTC, a significant 2-metre temperature difference, around 3-
187 4 °C, is apparent from 20th Century Reanalysis Project fields between the Po Valley



188 and the Liguria sea (Fig. 4a), as well as a significant 2-metre specific humidity
189 gradient (Fig. 4b). The temperature difference is also confirmed by the available
190 observations at 07 UTC provided the Italian Royal Central Office for Meteorology (Fig.
191 4c).

192
193

Fig. 4

194 These mesoscale features represent the necessary ingredients for the generation of a
195 back-building MCS offshore of the Liguria coastline, as observed in the 2010, 2011
196 and 2014 high impact weather events in this region (Parodi et al. 2012, Rebora et al.
197 2013, Fiori et al. 2014).

198 The back-building MCS hypothesis is supported by the 48-hour quantitative
199 precipitation estimates (QPEs) for the period 24th September 07UTC - 26th September
200 07UTC (Fig. 5). The raingauges (64) contributing to this map have been provided by
201 different datasets such as the European Climate Assessment & Dataset project (Klein
202 Tank et al. 2002, Klok and Klein Tank 2009), the KNMI Climate Explorer dataset
203 (Trouet and Van Oldenborgh 2013), the Italian Meteorological Society (SMI, Auer et
204 al. 2005), the Piedmont Region climatological dataset (Cortemiglia 1999), and the
205 Chiavari Meteorological Observatory (Ansaloni 2006).

206
207

Fig. 5

208

209 The QPE map shows clearly a v-shaped elongated pattern, very similar to the ones
210 observed for the aforementioned events in Liguria. Based on historical information on
211 sub-daily rain rates, it can be estimated that during the most intense phase of the
212 event, the rainfall depths reached up to 400 mm in approximately 4 hours (7-11 UTC
213 on September 25th) in some raingauges (Faccini et al. 2009): as a consequence of this
214 intense and highly localized rainfall the coastal cities of Rapallo, Santa Margherita
215 Ligure, Chiavari and San Fruttuoso suffered very serious damages (Fig. 6), with a
216 death toll around 25-30 people. Interestingly, as in the case of the Genoa 2014 event
217 (Lagasio et al. 2016) a very intense lightning activity was documented by the Italian
218 Royal Central Office for Meteorology (Fig. 7).

219
220

Fig. 6

221

Fig. 7

222

223 3. WRF-ARW model simulations

224

225 The model simulations have been performed using the Advanced Research Weather
226 Research and Forecasting Model (hereafter as ARW-WRF, version 3.4.1). Initial and
227 boundary conditions were provided by the 20th Century Reanalysis Project Version
228 version 2c (Compo et al. 2006, Compo et al. 2011) The ARW-WRF model was applied
229 for each of the 56 members of the ensemble provided by the 20th Century Reanalysis
230 Project database.

231 The ARW-WRF model is configured for this case study based on the results achieved in
232 the WRF modelling of the Genoa 2011 and Genoa 2014 v-shape convective structures
233 (Fiori et al. 2011, Fiori et al., 2015). Three nested domains (Fig. 8), centered on the
234 Liguria region, were used with the outer nest d01 using 25 km horizontal grid spacing



235 (61x55 grid points), the middle nest d02 using 5 km grid spacing (181x201 grid
236 points) and the innermost nest d03 using 1 km grid spacing (526x526 grid points).
237 The benefits of a high number of vertical levels have been demonstrated in Fiori et al.
238 (2014), and thus the same higher number of vertical levels (84) is adopted in this
239 study. Since the grid-spacing ranges from the regional modelling limit (25 km) down
240 to the cloud resolving one (1 km), two different strategies have been adopted with
241 regard to convection parameterization. For the domain d01 we adopted the new
242 simplified Arakawa–Schubert scheme (Han and Pan 2011) as it is also used by the
243 20th Century Reanalysis Project with 2.0° grid spacing. Conversely, a completely
244 explicit treatment of convective processes has been carried out on the d02-5 km and
245 d03-1 km domains (Fiori et al., 2014).

246

247

Fig. 8

248

249 The double-Moment Thompson et al. (2008) scheme for microphysical processes has
250 been adopted: this scheme takes into account ice species processes, whose relevance
251 in this case study is confirmed by the intense lightning activity observed during the
252 event, by modelling explicitly the spatio-temporal evolution of the intercept parameter
253 N_i for cloud ice. Furthermore, the Thompson scheme was shown to be the best
254 performing for the Genoa 2011 and Genoa 2014 studies (Fiori et al. 2014 and 2015).
255 With regard to the results in Fiori et al. (2014) about the role of the prescribed
256 number of initial cloud droplets $-Nt_c-$ created upon autoconversion of water vapour to
257 cloud water and directly connected to peak rainfall amounts, a maritime value
258 corresponding to a Nt_c of $25 \cdot 10^6 \text{ m}^{-3}$ has been adopted.

259 It is important to highlight that the availability of the 56 members ensemble is a key
260 strength in the present study, which enables estimates of uncertainties associated
261 with dynamical downscaling down to the WRF d03-1 km domain.

262

4. Results and discussion

263

264 A fundamental ingredient for the occurrence of back-building MCSs is the presence of
265 a persistent and robust convergence line: the availability of a large 1 km WRF
266 dynamically downscaled ensemble (56 members) allows the exploration of how many
267 members produce such a convergence line over the northern part of the Liguria sea
268 region where most of such MCSs form (Rebora et al. 2013). A convergence line is
269 here classified as persistent and robust if the minimum value of the divergence within
270 the study area is less than $-7 \cdot 10^{-3} \text{ s}^{-1}$ for at least 4 hours in a row. The divergence
271 threshold equal to $-7 \cdot 10^{-3} \text{ s}^{-1}$ corresponds to the 99.95% percentile of the divergence
272 values computed in every grid point within the region 7.50-10.25E / 43.75-44.50N in
273 Fig. 8 for each ensemble member in the period 12UTC 24th September – 00UTC 26th
274 September (with a 30-minute time resolution).
275

276

277 Using the above threshold, 17 of the 56 WRF-ARW runs exhibit a persistent and
278 robust convergence line in the considered period. In particular, the time series of
279 divergence for four members (1, 13, 22, and 37 respectively) show that the minimum
280 is reached (Fig. 9 at approximately at the same time hourly QPF exceeds 50 mm/h
281 (Fig. 10, panels a-d, and g-l, members 1 and 13, Fig. 13, panels a-d, and g-l,
282 members 22 and 37; the other 13 members are not shown as they behave very
283 similarly). The four representative members exhibit also large QPFs over the whole 36
284 hours of the simulations (Fig. 10, panels f and n, members 1 and 13, Fig. 11, panels f



285 and n, members 22 and 37), even though significant differences both in the total
286 amount and in the spatial distribution are found. Significant values of the Lightning
287 Potential Index (LPI, Yair et al. 2010), in good agreement with the observations of the
288 Italian Royal Central Office for Meteorology are shown in Fig. 10 (panels e and m,
289 members 1 and 13) and Fig. 11, (panels e and m, members 22 and 37).

290

291

Fig. 9

292

Fig. 10

293

Fig. 11

294

295 Yet, most of the back-building MCS-producing members are affected by a non-
296 negligible location error (see panel 6 of Figures 10 and 11 for the four selected
297 members) with respect to the observed daily rainfall map (Fig. 5). This feature is
298 largely due to a predominance of the south-easterly wind component over the north-
299 westerly one (coming from Po Valley), thus pushing the convergence line too north-
300 westwards, close to the western Liguria coastline. This discrepancy is explained by the
301 highly localized spatio-temporal nature of this event, by the comparatively low spatial
302 density of the surface pressure stations assimilated by the 20th Century Reanalysis
303 Project over the western Mediterranean region (Fig. 12) and by the relatively coarse
304 characteristics (2.0° grid spacing, and 6-hourly temporal resolution) of the 20th
305 Century Reanalysis Project forcing initial and boundary conditions data. For instance,
306 the primary wind convergence area over the sea and the inland area affected by the
307 rainfall (6.5-10.5° E / 43.5-45.5° N) is represented by only a few (2-3) 20th Century
308 Reanalysis Project grid points.

309

310

Fig. 12

311

312 To quantitatively examine precipitation errors for each WRF-ARW ensemble member,
313 a bias and mean absolute error (MAE) analysis of the 36 hour (12UTC 24/09 – 00UTC
314 26/09) QPF versus the 48 hour QPE (07UTC 24/09 – 07UTC 26/09) is undertaken by
315 comparing the available 64 raingauges with the nearest grid points of the d03-1 km.
316 The use of different time periods for QPE and QPF is not an issue as most of the
317 observed precipitation reported for Liguria fell in a time span encompassed in the run
318 time of the simulations. The results (Fig. 13) show that most of the 56 WRF members
319 have a negative BIAS of roughly 10-40 mm, largely explained by the ensemble
320 widespread underestimation of the extreme rainfall depths over the coastal cities of
321 Santa Margherita Ligure, Rapallo, and Chiavari. The 17 selected members (red
322 markers) show an average BIAS of -22 mm and a MAE of 40 mm, while the remaining
323 39 members have an average BIAS of -31 mm and a MAE of 42 mm. Also for the 17
324 selected members, the BIAS is largely explained by the stations mostly affected by
325 the MCS and it reduces to -8 mm when Chiavari, Cervara and S. Margherita Ligure are
326 excluded from the comparison.

327

328

Fig. 13

329

330 Because traditional verification measures applied to QPF are greatly influenced by
331 location errors, a deeper understanding of QPF performance in the WRF ensemble is
332 gained by performing object based verification using the Method for Object-based
333 Diagnostic Evaluation (MODE, Davis et al. 2006a, 2006b), intended to reproduce a
334 human analyst's evaluation of the forecast performance. The MODE analysis is
335 performed using a multi-step automated process. A convolution filter is applied to the
336 raw field to identify the objects. When the objects are identified, some attributes



337 regarding geometrical features of the objects (such as location, size, aspect ratio and
338 complexity) and precipitation intensity (percentiles, etc.) are computed. These
339 attributes are used to merge objects within the same forecast/observation field, to
340 match forecast and observed objects and to summarize the performance of the
341 forecast by attribute comparison. Finally, the interest value combines in a total
342 interest function the attributes (the centroid distance, the boundary distance, the
343 convex hull distance, the orientation angle difference, the object area ratio, the
344 intersection divided by the union area ratio, the complexity ratio, and the intensity
345 ratio) computed in the object analysis, providing an indicator of the overall
346 performance of matching and merging between observed and simulated objects. In
347 the present study, the relative weight of each attribute used the default setting in MET
348 (Halley Gotway et. al. 2013). The displacement errors including centroid distance and
349 boundary distance were weighted the greatest in the calculation of total interest.
350

351 In our experiment we have empirically chosen the convolution disk radius and
352 convolution threshold, so that this choice would recognize precipitation areas (at least
353 roughly 50x50 km or so) similar to what a human would identify. For each WRF
354 ensemble member the 36-hour (12UTC 24/09 – 00UTC 26/09) QPF is compared with
355 the 48-hour QPE (07UTC 24/09 – 07UTC 26/09), both bilinearly interpolated to the
356 same 10 km grid. This grid spacing represents a good compromise between the native
357 1 km WRF grid spacing and the 40 km average distance between the available 64
358 raingauges. After a set of experiments, we fixed the value of the convolution radius to
359 one grid point and the threshold of the convoluted field to 75 mm. Twelve members
360 out of the 17 members selected using the minimum divergence criterion show
361 significant values (above 0.8) of the total interest function. This value is slightly
362 higher than the default one (0.7) used by MODE to match paired objects, in order to
363 restrict our analysis to the best simulated events. Selected members 1, 13, 22 and 37
364 (Fig. 14) have total interest values above 0.93 (close to 1 is good) and their paired
365 clusters distance, namely the distance between centroids of observed and simulated
366 rain regions, is around 100 km. Furthermore, the area ratio -that provides an
367 objective measure of whether there is an over- or underprediction of the areal extent
368 of the forecast- ranges between 0.80 and 1.1, suggesting a reasonable agreement
369 with observations. However, the differences are larger for the median (50th percentile)
370 and near-peak (90th percentile) rainfall values: the predicted values are 30% lower
371 than the observed ones, suggesting an overall underestimation of the intense rainfall
372 observed.

373

374

375

Fig. 14

376 5. Conclusions

377

378 Highly localized and persistent back-building MCSs represent one of the most
379 dangerous flash-flood producing storms in the north-western Mediterranean area. A
380 historic extreme precipitation event occurring over Liguria on September 1915, which
381 seems to be due to one of these systems, was investigated in this paper both by
382 means of a large collection of observational data and by means of atmospheric
383 simulations performed using the WRF model forced by an ensemble of reanalysis
384 fields from the 20th Century Reanalysis Project.

385 The results show that the simulated circulation features are consistent with the
386 hypothesis of a highly localized back-building MCS over Liguria sea, and that the WRF
387 runs -driven by a significant fraction of the members of the 20th Century Reanalysis



388 Project ensemble- produce fields that are in reasonable agreement with the observed
389 data.

390 The proposed approach was to focus only on the WRF runs showing strong
391 convergence so as to get the best depiction of the event. Thus, we suggest that, when
392 using datasets such as the 20th Century Reanalysis Project, it is important to consider
393 that the physics/dynamics are likely to play a role in the events of interest, and to
394 follow a similar technique to selectively use the Reanalysis ensemble members best
395 displaying the key physics/dynamics of the event. Future work should test further an
396 approach like this one to get a better understanding of how well the same
397 convergence detection approach in regional climate model simulations of past and
398 future climate (e.g. Pieri et al. 2015 at cloud-permitting grid spacing) can quantify
399 possible changes in back-building MCS precipitation processes.

400 On the data collection side, this study showed that in addition to the use of Reanalysis
401 products, other sources of data, such as newspapers, photographs, and historical
402 meteorological bulletins can be essential sources of knowledge. Focusing on historical
403 meteorological bulletins, future work on this particular case and similar ones occurring
404 along the north-western Mediterranean coastline will explore the use of bogus
405 observations or other preprocessing techniques to alter lower tropospheric conditions
406 at model initialization time to better match actual observations, which may result in a
407 better location of the convergence line and consequently simulation of the
408 precipitation event.

409

410 **6. Acknowledgments**

411

412 This work was supported by the Italian Civil Protection Department and by the
413 Regione Liguria. The ground based observations were provided by Italian Civil
414 Protection Department and the Ligurian Environmental Agency. The raingauge data
415 were courtesy of the European Climate Assessment & Dataset project, the KNMI
416 Climate Explorer dataset, the Italian Meteorological Society, Piedmont Region
417 climatological dataset, and the Chiavari Meteorological Observatory. Antonio Parodi
418 would like also to acknowledge the support of the FP7 DRIHM (Distributed Research
419 Infrastructure for Hydro-Meteorology, 2011-2015) project (contract number 283568).
420 Thanks are due to the CINECA, where the numerical simulations were performed on
421 the Galileo System, Project-ID: SCENE. W. Gallus appreciates the opportunity for a
422 research visit at the University of Milan.

423

424

425

426 **7. References**

427

428 Alpert, P., Ben-Gai, T., Baharad, A., Benjamini, Y., Yekutieli, D., Colacino, M., ... &
429 Michaelides, S. (2002). The paradoxical increase of Mediterranean extreme daily
430 rainfall in spite of decrease in total values. *Geophysical research letters*, 29(11).

431

432 Ansaloni, A. (2006). The Observatory at Chiavari, Italy: its history and museum.
433 *Weather*, 61(10), 283-285.

434

435 Auer, I., Böhm, R., Jurković, A., Orlik, A., Potzmann, R., Schöner, W., ... & Briffa, K.
436 (2005). A new instrumental precipitation dataset for the greater alpine region for the
437 period 1800–2002. *International Journal of Climatology*, 25(2), 139-166.

438



- 439 Barriendos, M., Coeur, D., Lang, M., Llasat, M. C., Naulet, R., Lemaître, D., & Barrera,
440 A. (2003). Stationarity analysis of historical flood series in France and Spain (14th-
441 20th centuries). *Natural Hazards and Earth System Science*, 3(6), 583-592.
442
- 443 Barriendos, M., & Rodrigo, F. S. (2006). Study of historical flood events on Spanish
444 rivers using documentary data. *Hydrological Sciences Journal*, 51(5), 765-783.
445
- 446 Boni, G., Parodi, A., & Rudari, R. (2006). Extreme rainfall events: Learning from
447 raingauge time series. *Journal of hydrology*, 327(3), 304-314.
448
- 449 Brugnara, Y., Brunetti, M., Maugeri, M., Nanni, T., & Simolo, C. (2012). High-
450 resolution analysis of daily precipitation trends in the central Alps over the last
451 century. *International Journal of Climatology*, 32(9), 1406-1422.
452
- 453 Brunet, M., Jones, P. D., Sigró, J., Saladié, O., Aguilar, E., Moberg, A., ... & López, D.
454 (2007). Temporal and spatial temperature variability and change over Spain during
455 1850–2005. *Journal of Geophysical Research: Atmospheres*, 112(D12).
456
- 457 Brunetti, M., Maugeri, M., & Nanni, T. (2001). Changes in total precipitation, rainy
458 days and extreme events in northeastern Italy. *International Journal of Climatology*,
459 21(7), 861-871.
460
- 461 Brunetti, M., Buffoni, L., Mangianti, F., Maugeri, M., & Nanni, T. (2004). Temperature,
462 precipitation and extreme events during the last century in Italy. *Global and planetary
463 change*, 40(1), 141-149.
464
- 465 Brunetti, M., Caloiero, T., Coscarelli, R., Gullà, G., Nanni, T., & Simolo, C. (2012).
466 Precipitation variability and change in the Calabria region (Italy) from a high
467 resolution daily dataset. *International Journal of Climatology*, 32(1), 57-73.
468
- 469 Cassola, F., Ferrari, F., Mazzino, A., & Miglietta, M. M. (2016). The role of the sea on
470 the flash floods events over Liguria (northwestern Italy). *Geophysical Research
471 Letters*, 43(7), 3534-3542.
472
- 473 Compo, G. P., Whitaker, J. S., & Sardeshmukh, P. D. (2006). Feasibility of a 100-year
474 reanalysis using only surface pressure data. *Bulletin of the American Meteorological
475 Society*, 87(2), 175-190.
476
- 477 Compo, G. P., Whitaker, J. S., Sardeshmukh, P. D., Matsui, N., Allan, R. J., Yin, X., ...
478 & Worley, S. J. (2011). The twentieth century reanalysis project. *Quarterly Journal of
479 the Royal Meteorological Society*, 137(654), 1-28.
480
- 481 Compo, G. P., Sardeshmukh, P. D., Whitaker, J. S., Brohan, P., Jones, P. D., & McColl,
482 C. (2013). Independent confirmation of global land warming without the use of station
483 temperatures. *Geophysical Research Letters*, 40(12), 3170-3174.
484
- 485 Cortemiglia, G. C. (1999). Serie climatiche ultracentenarie (con allegato CD ROM).
486 Collana Studi Climatologici in Piemonte, Regione Piemonte, 3, 1-92.
487
- 488 Cram, T. A., Compo, G. P., Yin, X., Allan, R. J., McColl, C., Vose, R. S., ... &
489 Bessemoulin, P. (2015). The international surface pressure databank version 2.
490 *Geoscience Data Journal*, 2(1), 31-46.
491



- 492 Davis, C., B. Brown, and R. Bullock, 2006a: Object-based verification of precipitation
493 forecasts. Part I: Methods and application to mesoscale rain areas. *Mon. Wea. Rev.*,
494 134, 1772–1784.
495
- 496 Davis, C., B. Brown, and R. Bullock, 2006b: Object-based verification of precipitation
497 forecasts. Part II: Application to convective rain systems. *Mon. Wea. Rev.*, 134, 1785–
498 1795.
499
- 500 Faccini, F., Piccazzo, M., & Robbiano, A. (2009). Natural hazards in San Fruttuoso of
501 Camogli (Portofino Park, Italy): a case study of a debris flow in a coastal environment.
502 *Bollettino della Societa Geologica Italiana*, 128(3), 641-654.
503
- 504 Duffourg, F., Nuissier, O., Ducrocq, V., Flamant, C., Chazette, P., Delano, J., ... &
505 Legain, D. (2015). Offshore deep convection initiation and maintenance during IOP16a
506 Offshore deep convection initiation and maintenance during HyMeX IOP 16a heavy
507 precipitation event. *Quarterly Journal of the Royal Meteorological Society*.
508
- 509 European Environmental Agency (2015), SOER 2015 — The European environment —
510 state and outlook 2015 A comprehensive assessment of the European environment's
511 state, trends and prospects, in a global context.
512
- 513 Fiori, E., Comellas, A., Molini, L., Rebora, N., Siccardi, F., Gochis, D. J., ... & Parodi, A.
514 (2014). Analysis and hindcast simulations of an extreme rainfall event in the
515 Mediterranean area: The Genoa 2011 case. *Atmospheric Research*, 138, 13-29.
516
- 517 Fiori, E., Ferraris, L., Molini, L., Siccardi, F., Kranzlmüller, D., Parodi, A. (2015).
518 Morphology of the triggering and evolution of a micro- α convective system in the
519 Mediterranean Sea. *Quarterly Journal of the Royal Meteorological Society*, submitted.
520
- 521 Gaume, E., Bain, V., Bernardara, P., Newinger, O., Barbuc, M., Bateman, A., ... &
522 Daliakopoulos, I. (2009). A compilation of data on European flash floods. *Journal of*
523 *Hydrology*, 367(1), 70-78.
524
- 525 Giese, B. S., Seidel, H. F., Compo, G. P., & Sardeshmukh, P. D. (2016). An ensemble
526 of ocean reanalyses for 1815–2013 with sparse observational input. *Journal of*
527 *Geophysical Research: Oceans*.
528
- 529 Giorgi, F., & Lionello, P. (2008). Climate change projections for the Mediterranean
530 region. *Global and Planetary Change*, 63(2), 90-104.
531
- 532 Grasso, V., & Crisci, A. (2016). Codified hashtags for weather warning on Twitter: an
533 Italian case study. *PLoS currents*, 8.
534
- 535 Halley Gotway, J., and Coauthors (2013). Model Evaluation Tools version 4.1
536 (METv4.1): User's guide 4.1. Developmental Testbed Center Rep., 226 pp. [Available
537 online at http://www.dtcenter.org/met/users/docs/users_guide/MET_Users_Guide_v4.1.pdf.]
538
539
- 540 Han, J., & Pan, H. L. (2011). Revision of convection and vertical diffusion schemes in
541 the NCEP global forecast system. *Weather and Forecasting*, 26(4), 520-533.
542
- 543 Hirahara, S., Ishii, M., & Fukuda, Y. (2014). Centennial-scale sea surface temperature
544 analysis and its uncertainty. *Journal of Climate*, 27(1), 57-75.



- 545
546 Klein Tank, A. M. G., Wijngaard, J. B., Können, G. P., Böhm, R., Demarée, G.,
547 Gocheva, A., ... & Heino, R. (2002). Daily dataset of 20th - century surface air
548 temperature and precipitation series for the European Climate Assessment.
549 *International journal of climatology*, 22(12), 1441-1453.
- 550
551 Klok, E. J., & Klein Tank, A. M. G. (2009). Updated and extended European dataset of
552 daily climate observations. *International Journal of Climatology*, 29(8), 1182-1191.
- 553
554 Kioutsoukis, I., Melas, D., & Zerefos, C. (2010). Statistical assessment of changes in
555 climate extremes over Greece (1955–2002). *International Journal of Climatology*,
556 30(11), 1723-1737.
- 557
558 Kostopoulou, E., & Jones, P. D. (2005). Assessment of climate extremes in the
559 Eastern Mediterranean. *Meteorology and Atmospheric Physics*, 89(1-4), 69-85.
- 560
561 Krueger, O., Schenk, F., Feser, F., & Weisse, R. (2013). Inconsistencies between long-
562 term trends in storminess derived from the 20CR reanalysis and observations. *Journal*
563 *of Climate*, 26(3), 868-874.
- 564
565 Yair, Y., Lynn, B., Price, C., Kotroni, V., Lagouvardos, K., Morin, E., ... & Llasat, M. D.
566 C. (2010). Predicting the potential for lightning activity in Mediterranean storms based
567 on the Weather Research and Forecasting (WRF) model dynamic and microphysical
568 fields. *Journal of Geophysical Research: Atmospheres*, 115(D4).
- 569
570 Lagasio, M., Fiori, E., Procopio, R., and Parodi, A. (2016). Lightning flash activity
571 indices as forecasting tool of high impact weather events over complex topography:
572 The Genoa 2014 critical case, in preparation.
- 573
574 Llasat, M. C., Barriendos, M., Barrera, A., & Rigo, T. (2005). Floods in Catalonia (NE
575 Spain) since the 14th century. Climatological and meteorological aspects from
576 historical documentary sources and old instrumental records. *Journal of Hydrology*,
577 313(1), 32-47.
- 578
579 Llasat, M. C., Marcos, R., Llasat-Botija, M., Gilabert, J., Turco, M., & Quintana-Seguí,
580 P. (2014). Flash flood evolution in North-Western Mediterranean. *Atmospheric*
581 *Research*, 149, 230-243.
- 582
583 Maugeri, M., Brunetti, M., Garzoglio, M., & Simolo, C. (2015). High-resolution analysis
584 of 1 day extreme precipitation in Sicily. *Natural Hazards and Earth System Science*,
585 15(10), 2347-2358.
- 586
587 Michaelis, A. C., & Lackmann, G. M. (2013), Numerical modelling of a historic storm:
588 Simulating the Blizzard of 1888. *Geophysical Res. Letters*, 40, 4092-4097.
- 589
590 Moberg, A., Jones, P. D., Lister, D., Walther, A., Brunet, M., Jacobeit, J., ... & Chen,
591 D. (2006). Indices for daily temperature and precipitation extremes in Europe
592 analyzed for the period 1901–2000. *Journal of Geophysical Research: Atmospheres*,
593 111(D22).
- 594
595 Parodi, A., Boni, G., Ferraris, L., Siccardi, F., Pagliara, P., Trovatore, E., ... &
596 Kranzmueller, D. (2012). The "perfect storm": From across the Atlantic to the hills of
597 Genoa. *Eos, Transactions American Geophysical Union*, 93(24), 225-226.



- 598
599 Pasquaré, F. A., & Oppizzi, P. (2012). How do the media affect public perception of
600 climate change and geohazards? An Italian case study. *Global and Planetary Change*,
601 90, 152-157.
602
- 603 Pieri, A. B., von Hardenberg, J., Parodi, A., & Provenzale, A. (2015). Sensitivity of
604 Precipitation Statistics to Resolution, Microphysics, and Convective Parameterization:
605 A Case Study with the High-Resolution WRF Climate Model over Europe. *Journal of*
606 *Hydrometeorology*, 16(4), 1857-1872.
607
- 608 Pinto, J. G., Ulbrich, S., Parodi, A., Rudari, R., Boni, G., & Ulbrich, U. (2013).
609 Identification and ranking of extraordinary rainfall events over Northwest Italy: The
610 role of Atlantic moisture. *Journal of Geophysical Research: Atmospheres*, 118(5),
611 2085-2097.
612
- 613 Reale, O., Feudale, L., & Turato, B. (2001). Evaporative moisture sources during a
614 sequence of floods in the Mediterranean region. *Geophysical research letters*, 28(10),
615 2085-2088.
616
- 617 Rebora, N., Molini, L., Casella, E., Comellas, A., Fiori, E., Pignone, F., ... & Parodi, A.
618 (2013). Extreme rainfall in the mediterranean: what can we learn from observations?.
619 *Journal of Hydrometeorology*, 14(3), 906-922.
620
- 621 Rodrigo, F. S. (2010). Changes in the probability of extreme daily precipitation
622 observed from 1951 to 2002 in the Iberian Peninsula. *International Journal of*
623 *Climatology*, 30(10), 1512-1525.
624
- 625 Schumacher, R. S., & Johnson, R. H. (2005). Organization and environmental
626 properties of extreme-rain-producing mesoscale convective systems. *Monthly weather*
627 *review*, 133(4), 961-976.
628
- 629 Silvestro, F., Rebora, N., Giannoni, F., Cavallo, A., & Ferraris, L. (2015). The flash
630 flood of the Bisagno Creek on 9th October 2014: An "unfortunate" combination of
631 spatial and temporal scales. *Journal of Hydrology*.
632
- 633 Silvestro, F., Rebora, N., Rossi, L., Dolia, D., Gabellani, S., Pignone, F., ... & Masciulli,
634 C. (2016). What if the 25 October 2011 event that struck Cinque Terre (Liguria) had
635 happened in Genoa, Italy? Flooding scenarios, hazard mapping and damage
636 estimation. *Natural Hazards and Earth System Sciences*, 16(8), 1737-1753.
637
- 638 Skamarock, W. C., Klemp, J. B., Dudhia, J., Gill, D. O., Barker, D. M., Wang, W., &
639 Powers, J. G. (2005). A description of the advanced research WRF version 2 (No.
640 NCAR/TN-468+ STR). National Center For Atmospheric Research Boulder Co
641 Mesoscale and Microscale Meteorology Div.
642
- 643 Stucki, P., Brönnimann, S., Martius, O., Welker, C., Rickli, R., Dierer, S., ... &
644 Sardeshmukh, P. D. (2015). Dynamical downscaling and loss modeling for the
645 reconstruction of historical weather extremes and their impacts: a severe Foehn storm
646 in 1925. *Bulletin of the American Meteorological Society*, 96(8), 1233-1241.
647
- 648 Thompson, G., Field, P. R., Rasmussen, R. M., & Hall, W. D. (2008). Explicit forecasts
649 of winter precipitation using an improved bulk microphysics scheme. Part II:



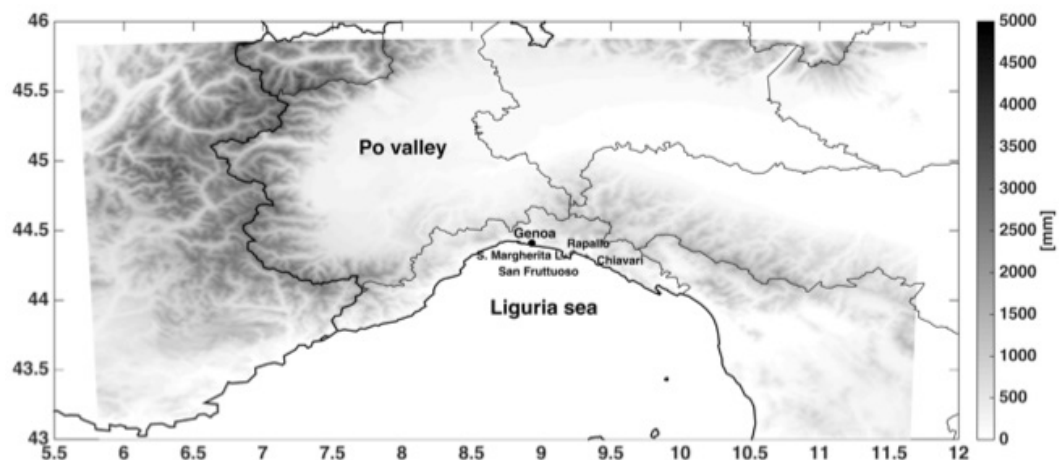
- 650 Implementation of a new snow parameterization. *Monthly Weather Review*, 136(12),
651 5095-5115.
- 652
- 653 Toreti, A., Xoplaki, E., Maraun, D., Kuglitsch, F. G., Wanner, H., & Luterbacher, J.
654 (2010). Characterisation of extreme winter precipitation in Mediterranean coastal sites
655 and associated anomalous atmospheric circulation patterns. *Nat. Hazards Earth Syst.*
656 *Sci*, 10(5), 1037-1050.
- 657
- 658 Toreti, A., Giannakaki, P., & Martius, O. (2015). Precipitation extremes in the
659 Mediterranean region and associated upper-level synoptic-scale flow structures.
660 *Climate Dynamics*, 1-17.
- 661
- 662 Trenberth, K. E. (2011). Changes in precipitation with climate change. *Climate*
663 *Research*, 47(1), 123.
- 664
- 665 Trouet, V., & Van Oldenborgh, G. J. (2013). KNMI Climate Explorer: a web-based
666 research tool for high-resolution paleoclimatology. *Tree-Ring Research*, 69(1), 3-13.
- 667
- 668 Ward, P. J., Jongman, B., Weiland, F. S., Bouwman, A., van Beek, R., Bierkens, M. F.,
669 ... & Winsemius, H. C. (2013). Assessing flood risk at the global scale: model setup,
670 results, and sensitivity. *Environmental research letters*, 8(4), 044019.
- 671
- 672 Whitaker, J. S., Compo, G. P., Wei, X., & Hamill, T. M. (2004). Reanalysis without
673 radiosondes using ensemble data assimilation. *Monthly Weather Review*, 132(5),
674 1190-1200.
- 675
- 676 Ulbrich, U., Lionello, P., Belušić, D., Jacobeit, J., Knippertz, P., Kuglitsch, F. G., ... &
677 Ziv, B. (2012). Climate of the Mediterranean: synoptic patterns, temperature,
678 precipitation, winds, and their extremes. In *The Climate of the Mediterranean Region-*
679 *From the Past to the Future*. Elsevier.
- 680
- 681 Van den Besselaar, E. J. M., Klein Tank, A. M. G., & Buishand, T. A. (2013). Trends in
682 European precipitation extremes over 1951–2010. *International Journal of*
683 *Climatology*, 33(12), 2682-2689.
- 684
- 685 Violante, C., Braca, G., Esposito, E., & Tranfaglia, G. (2016). The 9 September 2010
686 torrential rain and flash flood in the Dragone catchment, Atrani, Amalfi Coast
687 (southern Italy). *Natural Hazards and Earth System Sciences*, 16(2), 333-348
- 688
- 689
- 690
- 691
- 692
- 693
- 694
- 695
- 696
- 697
- 698
- 699



700 **Figures and figure captions**

701

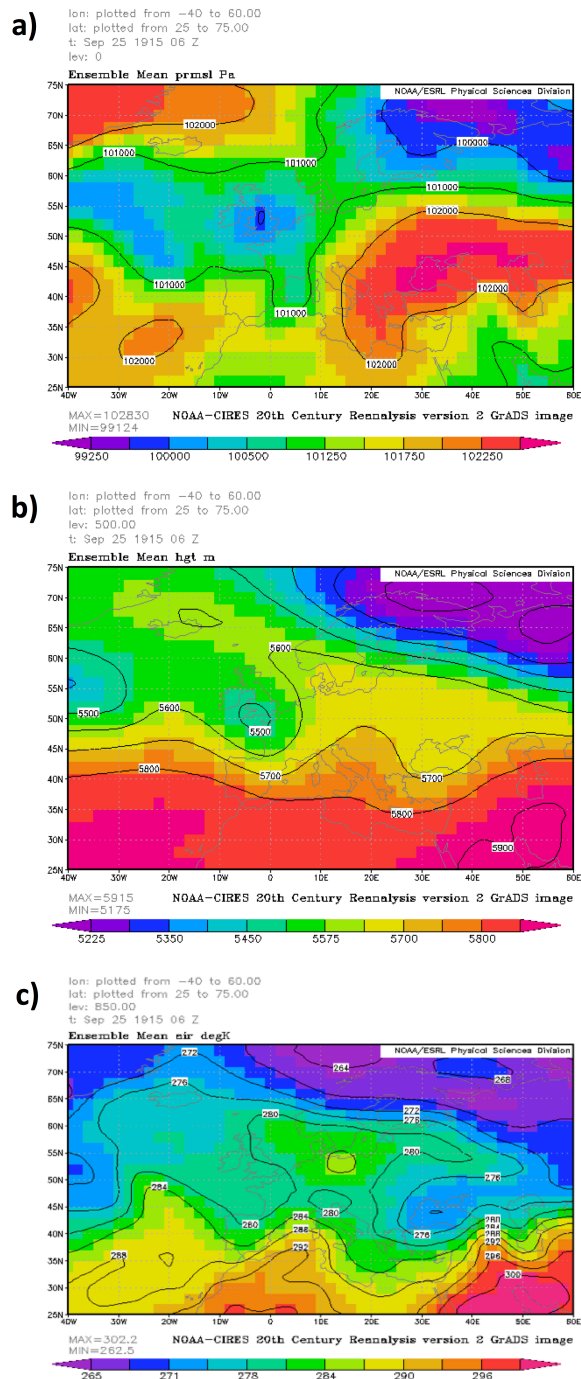
702



703

704 ***Figure 1: Study region and Liguria coastal cities affected by the September***
705 ***1915 event.***

706

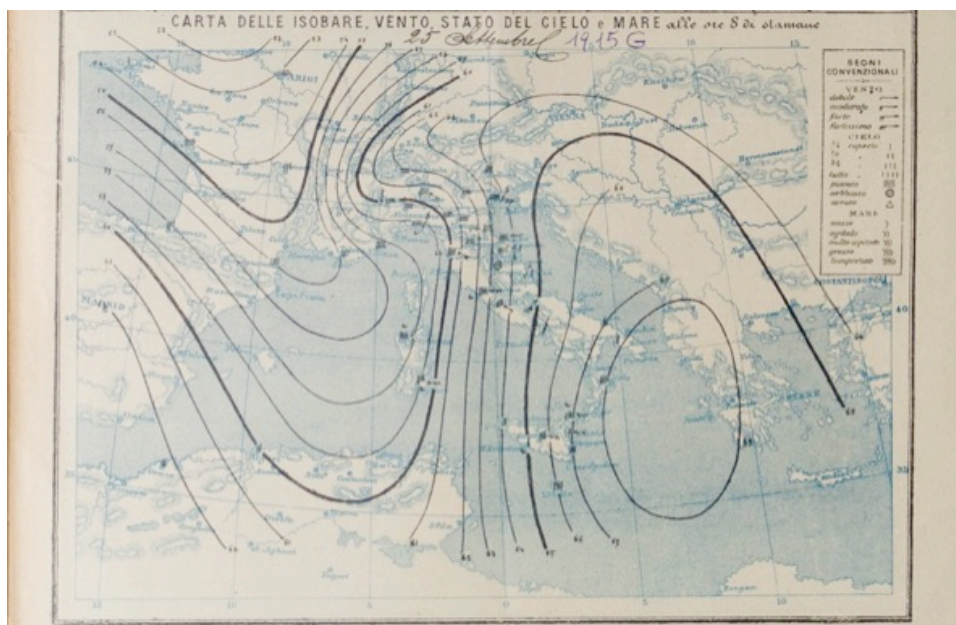


707
 708
 709
 710
 711

Figure 2: a) sea level pressure, b) 500 hPa geopotential, and c) 850 hPa temperature on 25th September 1915 06UTC (20th Century Reanalysis Project mean fields over the 56 ensemble members).

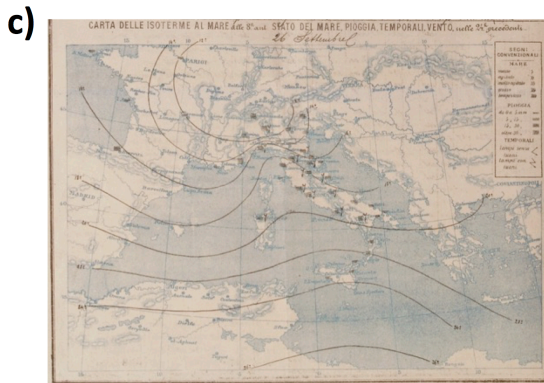
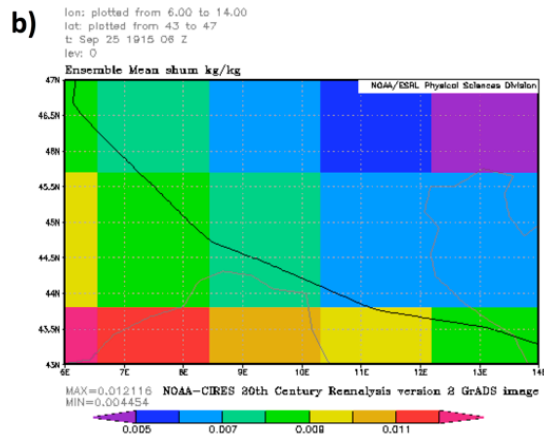
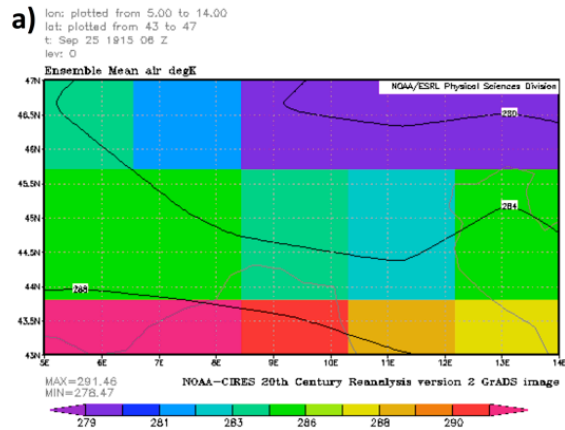


712



713
714
715
716

Figure 3: surface pressure isobars on 25th September 1915 at 07UTC, as provided by the Italian Royal Meteorological Service.



717

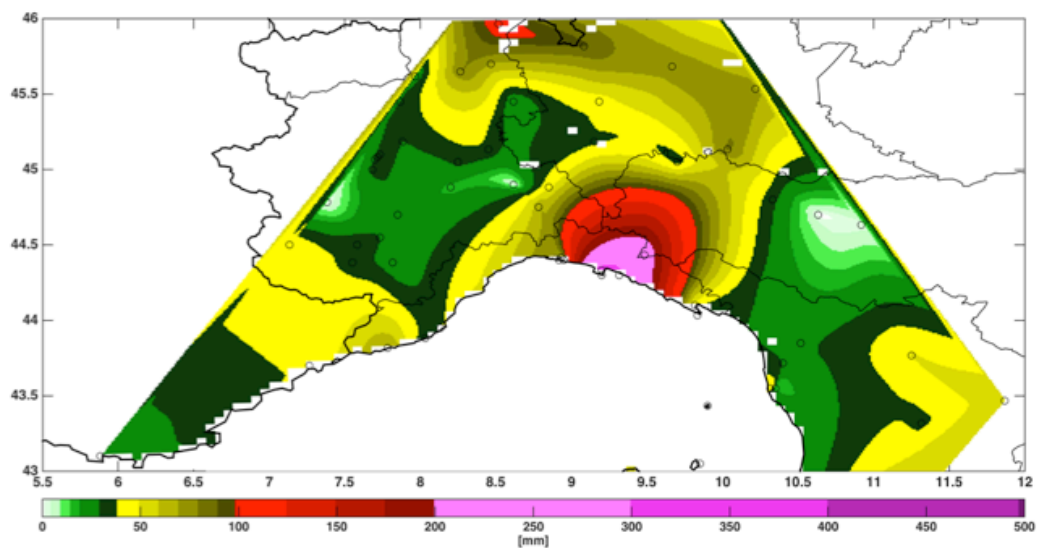
718

719 **Figure 4: a) 2 m temperature and b) 2 m specific humidity on 25th**
 720 **September 1915 06 UTC over the study region. (20th Century Reanalysis**
 721 **mean fields over the 56 ensemble members), c) surface temperature**
 722 **isotherms on 25th September 1915 at 07UTC, as provided by the Italian**
 723 **Royal Meteorological Service.**

724



725



726
727
728
729

Figure 5: quantitative precipitation estimates (QPE) for 24th September 07UTC - 26th September 1915 07UTC.



730
731



732



733
734
735

Figure 6: Rapallo flash-flood impacts on 25 september 1915 (Courtesy of real estate Agency Bozzo in Camogli).



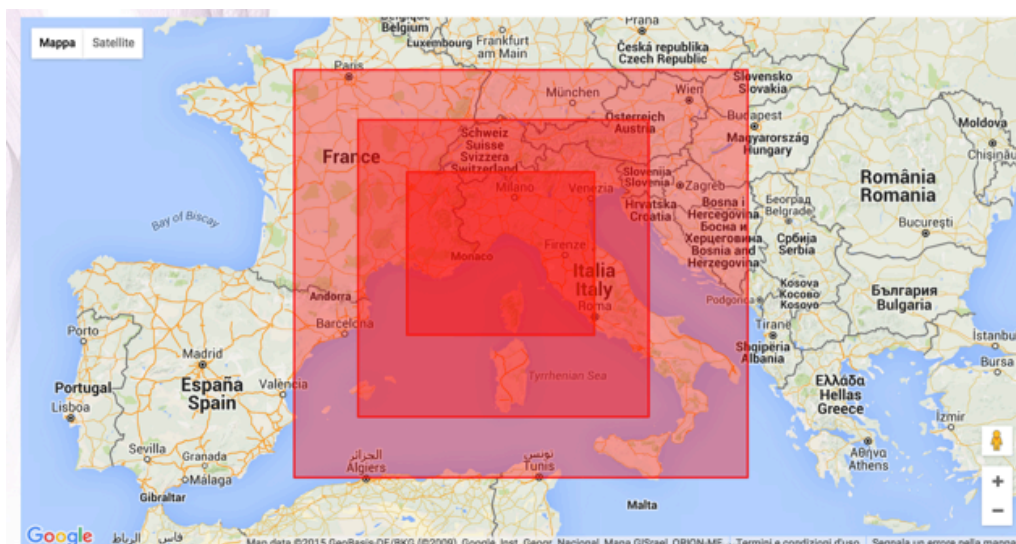
Città	Pressione barom. ridotta al mare 24 ore		Vento in barom.	Vento in forza o forza	Temperat. alle 8 ore in F.	Stato del cielo	Stato del mare	Nelle 24 ore			Osservazioni alle 21 ^h di sera				Osservazioni Diverse		
	Barom. Diff. in mm.	Barom. in mm.						Temperatura massima	Minimo	Umidità	Barom.	Temperatura	Umidità	Stato del cielo			
LIGURIA																	
Saint Remigio	525	-0.1	ca	-	17.0	5.0	1/2 cop.	18	17.0	18.0	dello	52.0	52.7	18.0	18	18	Notte tempest.
Saint Orens	526	+0.0	ca	-	17.0	2.0	1/2 cop.	18	17.0	18.0	cop.	52.0	52.5	18.0	18	18	Pann. fissa. Luce
Genova	535	-0.3	ca	-	17.0	1.0	1/2 cop.	18	17.0	18.0	"	52.0	52.1	18.0	18	18	St. fissa. Pan. f. L. Luce
Speria	544	+0.0	ca	-	17.0	2.0	1/2 cop.	18	17.0	18.0	"	52.0	52.5	18.0	18	18	St. fissa. Luce. Luce

736
 737
 738
 739

Figure 7: thunderstorms and lightning activity reports (red circle) on 25th September 1915, as provided by the Italian Royal Meteorological Service.



740

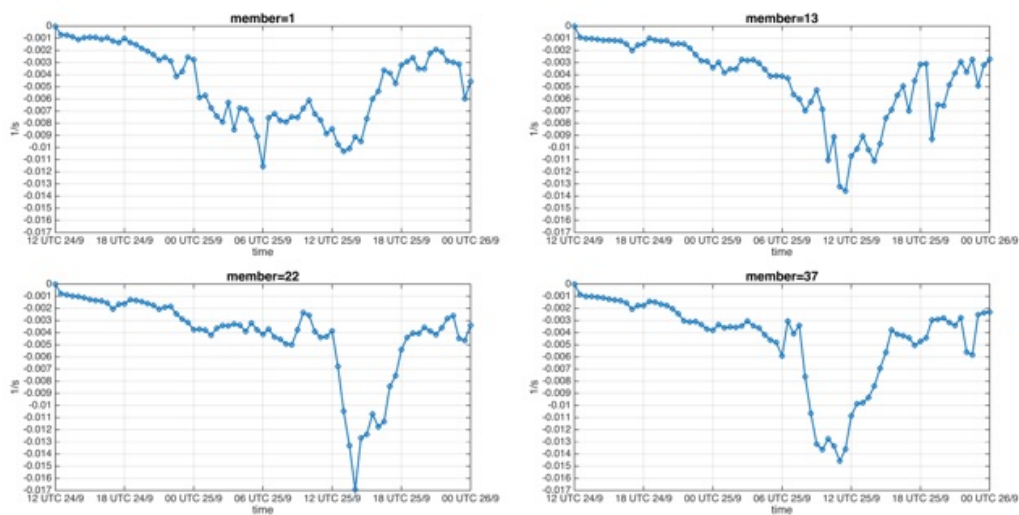


741
742
743
744

Figure 8: domains for the numerical simulations of the Genoa 1915 event. d01 ($\Delta=25$ km), d02 ($\Delta=5$ km) and d03 ($\Delta=1$ km).



745



746

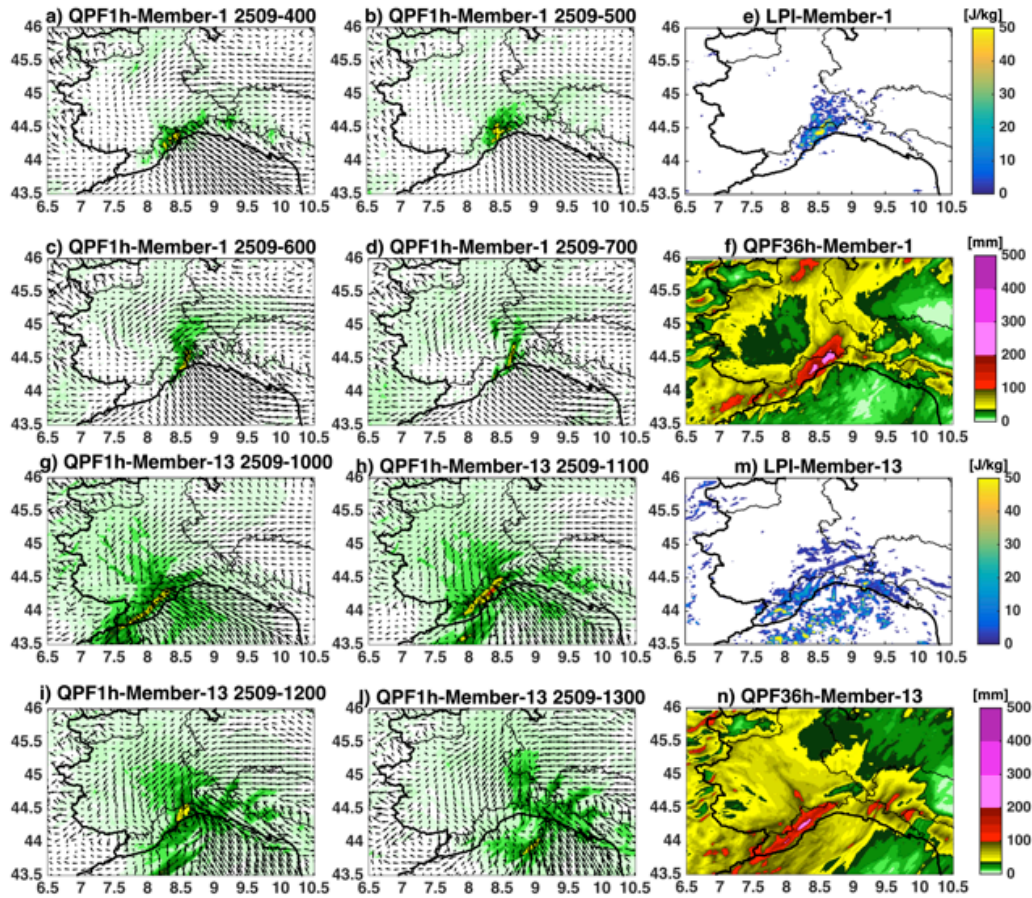
747

748

Figure 9: minimum divergence time series for members 1, 13, 22 and 37.

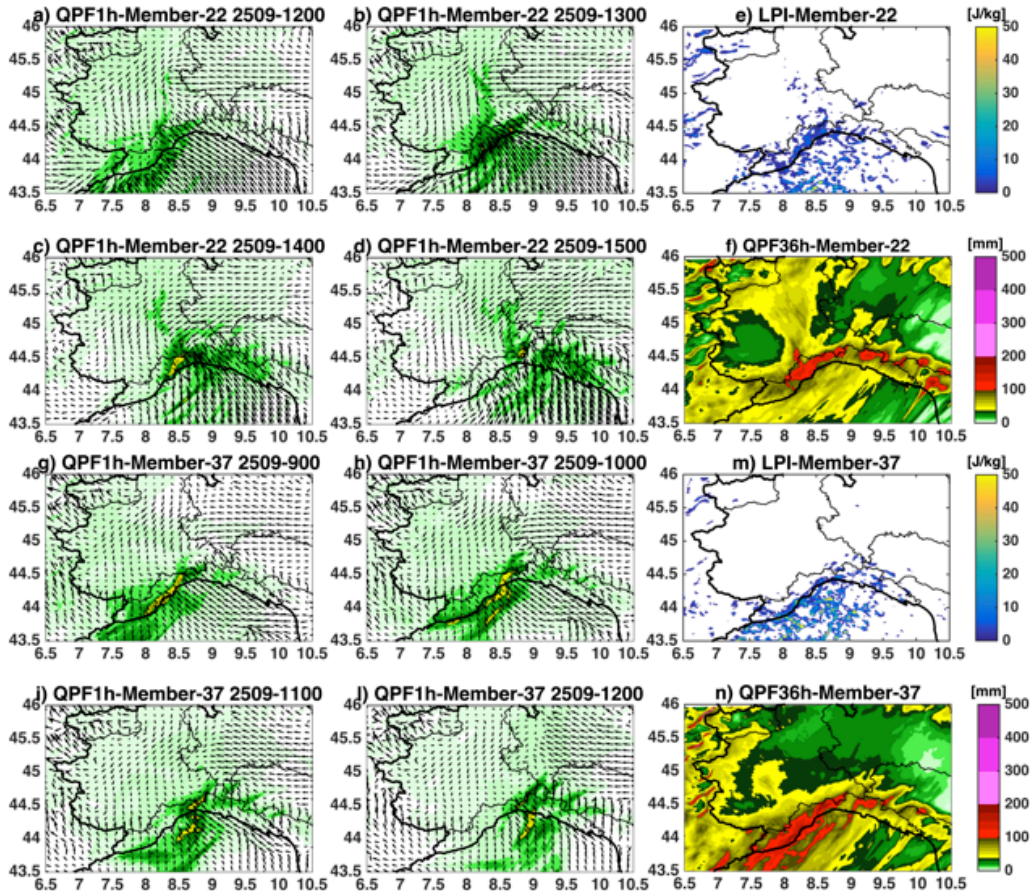
749

750



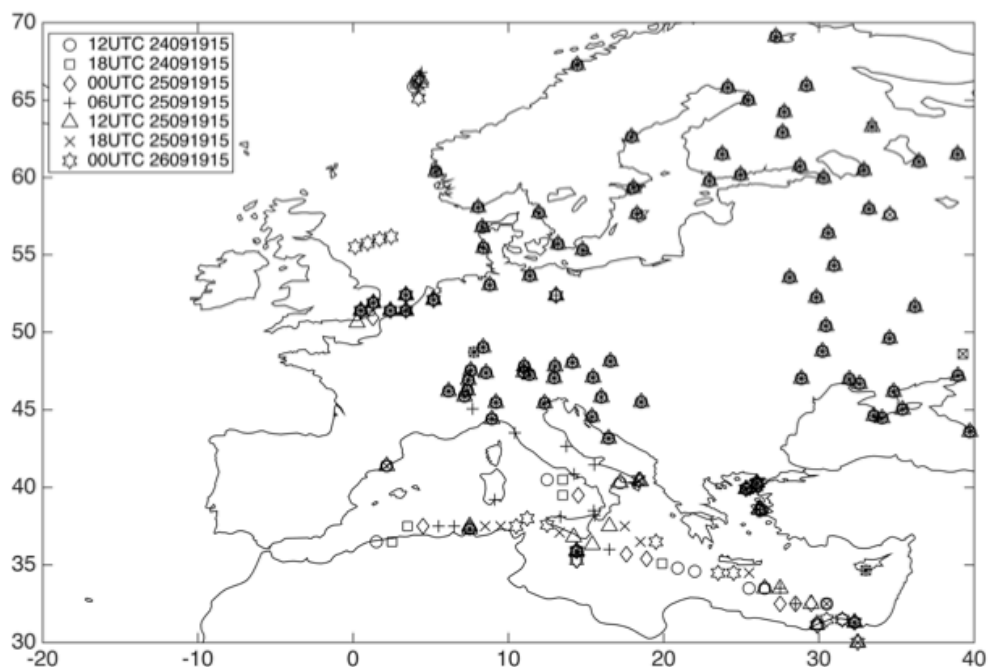
751
752
753
754
755
756
757
758

Figure 10: Panels a-d, and g-l show the hourly QPF and 10 m wind fields corresponding to the period with the minimum divergence values in Figure 11 for members 1, and 13. Panels e-f, and m-n show the Lightning Potential Index accumulated over the same 4 hours period, and the 36 hour QPF, respectively for members 1, and 13.



759
760
761
762
763
764
765
766
767
768
769
770
771
772
773
774
775
776
777

Figure 11: Panels a-d, and g-l show the hourly QPF and 10 m wind fields corresponding to the period with the minimum divergence values in Figure 11 for members 22, and 37. Panels e-f, and m-n show the Lightning Potential Index accumulated over the same 4 hours period, and the 36 hour QPF, respectively for members 22, and 37.

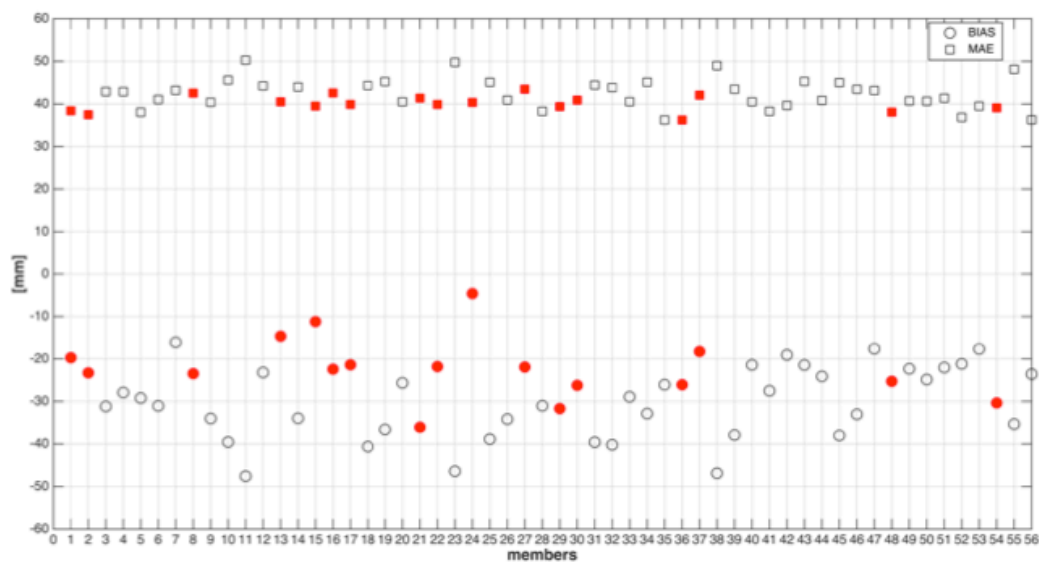


778
779
780
781

Figure 12: surface pressure stations assimilated every six hours in the period 12UTC 24th September 1915 - 00UTC 26th September 1915.



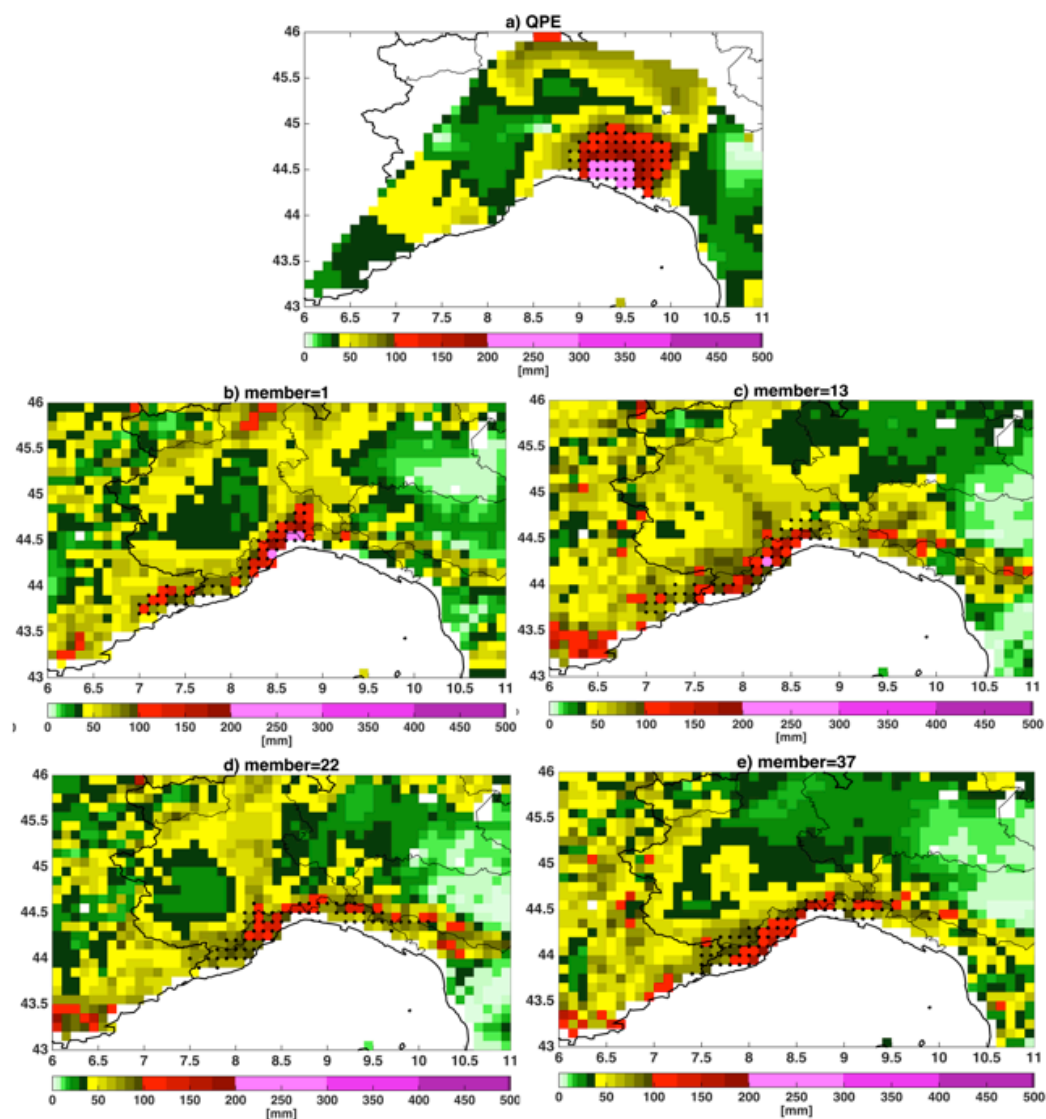
782
783



784
785
786
787
788

789
790
791

Figure 13: rainfall depth BIAS and MAE for each d03-1km WRF member. Red markers represent the 17 members producing robust and persisting convergence lines over the Liguria Sea.



792
793
794
795
796
797
798
799
800
801
802

Figure 14: QPE regridDED at 10 km grid spacing (panel a) and QPF from members 1 (panel b), 13 (panel c), 22 (panel d) and 37 (panel e), regridDED at 10 km grid spacing (lower panels). Dots identify the areas of paired clusters.